DESY 10–025 ISSN 0418-9833
March 2010

Inclusive b and $b\bar{b}$ production with quasi-multi-Regge kinematics at the Tevatron

B.A. Kniehl*

II. Institut für Theoretische Physik, Universität Hamburg,

Luruper Chaussee 149, 22761 Hamburg, Germany

V.A. Saleev† and A.V. Shipilova‡

Samara State University, Academic Pavlov Street 1, 443011 Samara, Russia

arXiv:1003.0346v2 [hep-ph] 23 Apr 2010

Abstract

We consider b-jet hadroproduction in the quasi-multi-Regge-kinematics approach based on the hypothesis of gluon and quark Reggeization in t-channel exchanges at high energies. The preliminary data on inclusive b-jet and $b\bar{b}$-dijet production taken by the CDF Collaboration at the Fermilab Tevatron are well described without adjusting parameters. We find the main contribution to inclusive b-jet production to be the scattering of a Reggeized gluon and a Reggeized b-quark to a b quark, which is described by the effective Reggeon-Reggeon-quark vertex. The main contribution to $b\bar{b}$-pair production arises from the scattering of two Reggeized gluons to a $b\bar{b}$ pair, which is described by the effective Reggeon-Reggeon-quark-quark vertex. Our analysis is based on the Kimber-Martin-Ryskin prescription for unintegrated gluon and quark distribution functions using as input the Martin-Roberts-Stirling-Thorne collinear parton distribution functions of the proton.

PACS numbers: 12.38.Bx, 12.39.St, 12.40.Nn, 13.85.-t

*Electronic address: kniehl@desy.de

†Electronic address: saleev@ssu.samara.ru

‡Electronic address: alexshipilova@ssu.samara.ru

I. INTRODUCTION

The study of b-jet and B-meson production at high-energy colliders, such as the Fermilab Tevatron and the CERN Large Hadron Collider, is of great interest for the test of perturbative quantum chromodynamics (QCD). The presence of a heavy b quark, with mass $m_b \gg \Lambda_{\rm QCD}$, where $\Lambda_{\rm QCD}$ is the asymptotic scale parameter of QCD, in such processes guarantees a large momentum transfer even if the transverse momentum of the produced b quark is small. Thus, the strong-coupling constant remains small in the processes discussed here, $\alpha_s(m_b) \lesssim 0.1$. The study of b-jet production should provide a more direct way to investigate gluon and quark interactions at small distances than that of B-meson production because, in the former case, there is no need for additional assumptions concerning the non-perturbative dynamics of the transition from a b quark to a B meson [1].

The total center-of-mass (CM) energy at the Tevatron, $\sqrt{S} = 1.96$ TeV in Run II, sufficiently exceeds the scale μ of the relevant hard processes, so that $\sqrt{S} \gg \mu \gg \Lambda_{\rm QCD}$. In such a high-energy regime, the contributions to the production cross section from subprocesses involving t-channel exchanges of partons (gluons and quarks) may become dominant. Then, the transverse momenta of the incoming partons and their off-shell properties can no longer be neglected, and we deal with *Reggeized* t-channel partons. In this so-called quasi-multi-Regge kinematics (QMRK), the particles (multi-Regge) or groups of particles (quasi-multi-Regge) produced in the collision are strongly separated in rapidity. In the case of inclusive b-jet production, this implies the following: a single b quark is produced in the central region of rapidity, while other particles, including a $\bar{b}$ quark, are produced at large rapidities. In the case of associated $b\bar{b}$-pair production in the central rapidity region, we also assume that there are no other particles in this region, so that the $b\bar{b}$ pair is considered as a quasi-multi-Regge pair of particles. The QMRK approach [2] is particularly appropriate for this kind of high-energy phenomenology. It is based on an effective quantum field theory implemented with the non-Abelian gauge-invariant action including fields of Reggeized gluons (Reggeons) [3] and Reggeized quarks [4].

In this paper, we apply the QMRK approach to various cross section distributions of b-jet hadroproduction. Specifically, we study the transverse-momentum distribution of single b-jet production and, for $b\bar{b}$-dijet production, the distributions in the leading-jet transverse energy, the dijet invariant mass, and the azimuthal angle between the b and $\bar{b}$ jets. We compare our

results with preliminary experimental data obtained by the CDF Collaboration [5, 6].

II. AMPLITUDES

We first study inclusive single b-jet production in $p\bar{p}$ collisions, working in the fixed-flavor-number scheme with $n_f = 5$ active quark flavors. To leading order (LO) in the QMRK approach, there is only one partonic subprocess, namely

$$Q_b(q_1) + R(q_2) \to b(k), \tag{1}$$

where Q_b and R are the Reggeized b quark and gluon, respectively, and the four-momenta are labeled as indicated in the parentheses. As the modulus of the transverse momentum $\vec{k}_T$ of the b quark, $k_T \geq 32$ GeV [5, 6], sufficiently exceeds its mass m_b, it is justified to assume beauty to be an active flavor in the proton. The effective vertex mediating subprocess (1) is given by [4]

$$C^b_{Q_b R}(q_1, q_2) = i\sqrt{4\pi\alpha_s}\, T^a \overline{u}(k) \gamma^{(-)\mu}(q_1, q_2) \Pi^{(+)}_\mu(q_2), \tag{2}$$

where T^a are the generators of the color gauge group SU(N_c) with $N_c = 3$ for QCD, $a = 1, \ldots, N_c^2 - 1$ is the color index of the Reggeized gluon, $k = q_1 + q_2$,

$$\begin{aligned} \gamma^{(\pm)}_\mu(q, p) &= \gamma_\mu + \not{q} \frac{n^\pm_\mu}{p^\pm}, \\ \Pi^{(\pm)}_\mu(q) &= -\frac{q^\mp n^\pm_\mu}{2\sqrt{-q^2}}, \end{aligned} \tag{3}$$

with $n^\pm_\mu = (1, 0, 0, \mp 1)$ in the CM frame and $q^\pm = q \cdot n^\pm$. In the following, we put $q^\mu_{1,2} = x^\mu_{1,2} + (0, \vec{q}_{1,2T}, 0)$, where P_1 and P_2 denote the four-momenta of the incoming proton and antiproton, and $\vec{q}_{1T}$ and $\vec{q}_{2T}$ the transverse momenta of the Reggeized b quark and gluon, respectively. We then have $\vec{k}^2_T = \vec{q}^2_{1T} + \vec{q}^2_{2T} + 2|\vec{q}_{1T}||\vec{q}_{2T}| \cos\phi_{12}$, where ϕ_{12} is the azimuthal angle enclosed between $\vec{q}_{1T}$ and $\vec{q}_{2T}$. The squared amplitude of subprocess (1) reads [7]:

$$\overline{|\mathcal{M}(Q_b R \to b)|^2} = \frac{2}{3}\pi\alpha_s \vec{k}^2_T. \tag{4}$$

At next-to-leading order (NLO) in the QMRK approach, the main contribution to inclusive b-quark production arises from the partonic subprocess

$$R(q_1) + R(q_2) \to b(k_1) + \bar{b}(k_2), \tag{5}$$

where the b and $\bar{b}$ quarks are produced close in rapidity. The contributions due to the other NLO processes, $R+Q_b \to g+b$, $Q_q+\bar{Q}_q \to b+\bar{b}$, and $Q_q(\bar{Q}_q)+Q_b \to q(\bar{q})+b$ are suppressed because, in the small-x region, the parton distribution function (PDF) of the gluon greatly exceeds the relevant quark PDFs. Using the effective Feynman rules of the QMRK approach, the effective vertex mediating subprocess (5) may be written in the following form:

$$\begin{aligned} C_{RR}^{b\bar{b}}(q_1,q_2) \;=\; & 4\pi\alpha_s \left[-\frac{1}{\hat{s}} f^{abc} T^c \overline{u}(k_1)\gamma_\mu v(k_2) C_{RR}^{g,\mu}(q_1,q_2) \right. \\ & + \frac{i}{\hat{t}} T^a T^b \overline{u}(k_1)\gamma^\mu (\not{k}_1 - \not{q}_1)\gamma^\nu v(k_2) \Pi_\mu^{(-)}(q_1)\Pi_\nu^{(+)}(q_2) \\ & \left. + \frac{i}{\hat{u}} T^b T^a \overline{u}(k_1)\gamma^\nu (\not{k}_1 - \not{q}_2)\gamma^\mu v(k_2) \Pi_\mu^{(-)}(q_1)\Pi_\nu^{(+)}(q_2) \right], \end{aligned} \tag{6}$$

where $\hat{s} = (q_1+q_2)^2$, $\hat{t} = (q_1-k_1)^2$, and $\hat{u} = (q_2-k_1)^2$ are the Mandelstam variables, a and b are the color indices of the Reggeized gluons carrying the four-momenta q_1 and q_2, respectively, and [2]

$$C_{RR}^{g,\mu}(q_1,q_2) = \frac{q_1^+ q_2^-}{2\sqrt{q_1^2 q_2^2}} \left[(q_1-q_2)^\mu + \frac{(n^+)^\mu}{q_1^+}\left(q_2^2 + q_1^+ q_2^-\right) - \frac{(n^-)^\mu}{q_2^-}\left(q_1^2 + q_1^+ q_2^-\right) \right] \tag{7}$$

is the effective Reggeon-Reggeon-gluon vertex with the color structure stripped off. The squared amplitude of subprocess (5) was obtained in Ref. [8]. It may be presented as the linear combination of an Abelian and a non-Abelian term, as

$$\overline{|\mathcal{M}(R+R \to b+\bar{b})|^2} = 256\pi^2\alpha_s^2 \left[\frac{1}{2N_c}\mathcal{M}_{\rm A} + \frac{N_c}{2(N_c^2-1)}\mathcal{M}_{\rm NA} \right], \tag{8}$$

where

$$\begin{aligned} \mathcal{M}_{\rm A} \;=\; & \frac{t_1 t_2}{\tilde{t}\tilde{u}} - \left(1 + \frac{\alpha_1\beta_2 S}{\tilde{u}} + \frac{\alpha_2\beta_1 S}{\tilde{t}}\right)^2, \\ \mathcal{M}_{\rm NA} \;=\; & \frac{2}{S^2}\left(\frac{\alpha_1\beta_2 S^2}{\tilde{u}} + \frac{S}{2} + \frac{\Delta}{\hat{s}}\right)\left(\frac{\alpha_2\beta_1 S^2}{\tilde{t}} + \frac{S}{2} - \frac{\Delta}{\hat{s}}\right) \\ & - \frac{t_1 t_2}{x_1 x_2 \hat{s}}\left[\left(\frac{1}{\tilde{t}} - \frac{1}{\tilde{u}}\right)(\alpha_1\beta_2 - \alpha_2\beta_1) + \frac{x_1 x_2 \hat{s}}{\tilde{t}\tilde{u}} - \frac{2}{S}\right], \\ \Delta \;=\; & \frac{S}{2}\left[\tilde{u} - \tilde{t} + 2S(\alpha_1\beta_2 - \alpha_2\beta_1) + t_1\frac{\beta_1-\beta_2}{\beta_1+\beta_2} - t_2\frac{\alpha_1-\alpha_2}{\alpha_1+\alpha_2}\right], \end{aligned} \tag{9}$$

$\tilde{t} = \hat{t} - m^2$, $\tilde{u} = \hat{u} - m^2$, $t_1 = -q_1^2$, $t_2 = -q_2^2$, $\alpha_1 = 2(k_1\cdot P_2)/S$, $\alpha_2 = 2(k_2\cdot P_2)/S$, $\beta_1 = 2(k_1\cdot P_1)/S$, and $\beta_2 = 2(k_2\cdot P_1)/S$, with $S = (P_1+P_2)^2$. To obtain the inclusive single b-jet production cross section, one needs to integrate the cross section of subprocess (5) over the $\bar{b}$-quark momentum.

At LO, $b\bar{b}$-dijet production receives contributions from both subprocess (5) and the annihilation of a Reggeized quark-antiquark pair,

$$Q_q(q_1) + \bar{Q}_q(q_2) \to b(k_1) + \bar{b}(k_2), \tag{10}$$

where $q = u, d, s, c, b$. Let us first consider the case $q \neq b$. Neglecting Reggeized-quark masses, the effective vertex mediating subprocess (10) is given by [4]:

$$C^{b\bar{b}}_{Q_q\bar{Q}_q}(q_1, q_2, k_1, k_2) = \frac{4\pi\alpha_s}{\hat{s}} T^a \bar{u}(k_1)\gamma^\mu v(k_2) \otimes T^a \gamma_\mu^{(+-)}(q_1, q_2), \tag{11}$$

where

$$\gamma_\mu^{(+-)}(q_1, q_2) = \gamma_\mu - \frac{\not{q}_1 n_\mu^-}{q_2^-} - \frac{\not{q}_2 n_\mu^+}{q_1^+}. \tag{12}$$

The squared amplitude of subprocess (10) is found to be

$$\overline{|\mathcal{M}(Q_q\bar{Q}_q \to b\bar{b})|^2} = \frac{64\pi^2\alpha_s^2}{9x_1x_2\hat{s}^2}\left(w_0 + w_1 S + w_2 S^2\right), \tag{13}$$

where

$$\begin{aligned}
w_0 &= x_1x_2\hat{s}\left(\tilde{t} + \tilde{u}\right), \\
w_1 &= -2x_2^2\alpha_1\alpha_2 t_2 - 2x_1^2\beta_1\beta_2 t_1 + x_1x_2\{(\alpha_2\beta_1 + \alpha_1\beta_2)(\hat{s} + t_1 + t_2) + x_1x_2(\hat{s} - 2m^2) \\
&\quad + x_1[\beta_1(t_1 + \tilde{u}) + \beta_2(t_1 + \tilde{t})] + x_2[\alpha_1(t_2 + \tilde{t}) + \alpha_2(t_2 + \tilde{u})]\}, \\
w_2 &= -2x_1x_2(\alpha_1\beta_2 - \alpha_2\beta_1)^2.
\end{aligned} \tag{14}$$

In the case of $q = b$, we have

$$\begin{aligned}
C^{b\bar{b}}_{Q_b\bar{Q}_b}(q_1, q_2, k_1, k_2) &= 4\pi\alpha_s\left[\frac{1}{\hat{s}} T^a \bar{u}(k_1)\gamma^\mu v(k_2) \otimes T^a \gamma_\mu^{(+-)}(q_1, q_2)\right. \\
&\quad \left. + \frac{1}{\hat{t}} T^a u(k_1)\gamma^{(-)\mu}(q_1, k_1 - q_1) \otimes T^a \gamma_\mu^{(+)}(-q_2, q_2 - k_2) v(k_2)\right].
\end{aligned} \tag{15}$$

The analytic expression for $\overline{|\mathcal{M}(Q_b\bar{Q}_b \to b\bar{b})|^2}$ is too lengthy to be presented here.

III. CROSS SECTIONS

Exploiting the hypothesis of high-energy factorization, we may write the hadronic cross sections $d\sigma$ as convolutions of partonic cross sections $d\hat{\sigma}$ with unintegrated PDFs Φ_a^h of

Reggeized partons a in the hadrons h. For the processes under consideration here, we have

$$\begin{aligned}
d\sigma(p\bar{p} \to bX) &= \int \frac{dx_1}{x_1} \int \frac{d^2q_{1T}}{\pi} \int \frac{dx_2}{x_2} \int \frac{d^2q_{2T}}{\pi} \left[\Phi_b^p(x_1, t_1, \mu^2)\Phi_g^{\bar{p}}(x_2, t_2, \mu^2)\right. \\
&\left. + \Phi_g^p(x_1, t_1, \mu^2)\Phi_b^{\bar{p}}(x_2, t_2, \mu^2)\right] d\hat{\sigma}(Q_b R \to b), \\
d\sigma(p\bar{p} \to b\bar{b}X) &= \int \frac{dx_1}{x_1} \int \frac{d^2q_{1T}}{\pi} \int \frac{dx_2}{x_2} \int \frac{d^2q_{2T}}{\pi} \left\{\Phi_g^p(x_1, t_1, \mu^2)\Phi_g^{\bar{p}}(x_2, t_2, \mu^2)\right. \\
&\times d\hat{\sigma}(RR \to b\bar{b}) + \sum_q \left[\Phi_q^p(x_1, t_1, \mu^2)\Phi_{\bar{q}}^{\bar{p}}(x_2, t_2, \mu^2)\right. \\
&\left.\left. + \Phi_{\bar{q}}^p(x_1, t_1, \mu^2)\Phi_q^{\bar{p}}(x_2, t_2, \mu^2)\right] d\hat{\sigma}(Q_q\bar{Q}_q \to b\bar{b})\right\}. \qquad (16)
\end{aligned}$$

The unintegrated PDFs $\Phi_a^h(x, t, \mu^2)$ are related to their collinear counterparts $F_a^h(x, \mu^2)$ by the normalization condition

$$xF_a^h(x, \mu^2) = \int^{\mu^2} dt\, \Phi_a^h(x, t, \mu^2), \qquad (17)$$

which yields the correct transition from formulas in the QMRK approach to those in the collinear parton model, where the transverse momenta of the partons are neglected. In our numerical analysis, we adopt the Kimber-Martin-Ryskin prescription [9] for unintegrated gluon and quark PDFs, using as input the Martin-Roberts-Stirling-Thorne collinear PDFs of the proton [10].

For the reader's convenience, we collect here compact formulas for the differential cross sections. In the case of inclusive single b-jet production, we have [11]

$$\begin{aligned}
\frac{d\sigma}{dk_T\, dy}(p\bar{p} \to bX) &= \frac{1}{k_T^3} \int d\phi_1 \int dt_1 \left[\Phi_b^p(x_1, t_1, \mu^2)\Phi_g^{\bar{p}}(x_2, t_2, \mu^2)\right. \\
&\left. + \Phi_g^p(x_1, t_1, \mu^2)\Phi_b^{\bar{p}}(x_2, t_2, \mu^2)\right] \overline{|\mathcal{M}(Q_b R \to b)|^2}, \qquad (18)
\end{aligned}$$

where y is the (pseudo)rapidity, ϕ_1 is the azimuthal angle enclosed between the vectors $\vec{q}_{1T}$ and $\vec{k}_T$,

$$x_{1,2} = \frac{k_T \exp(\pm y)}{\sqrt{S}}, \qquad t_2 = t_1 + k_T^2 - 2k_T\sqrt{t_1}\cos\phi_1. \qquad (19)$$

In the case of $b\bar{b}$-dijet production, we have

$$\begin{aligned}
\frac{d\sigma(p\bar{p} \to b\bar{b}X)}{dk_{1T}\, dy_1\, dk_{2T}\, dy_2\, d\Delta\phi} &= \frac{k_{1T}k_{2T}}{16\pi^3 S^2} \int dt_1 \int d\phi_1 \frac{1}{(x_1x_2)^2} \left\{\Phi_g^p(x_1, t_1, \mu^2)\Phi_g^{\bar{p}}(x_2, t_2, \mu^2)\right. \\
&\times \overline{|\mathcal{M}(RR \to b\bar{b})|^2} + \sum_q \left[\Phi_q^p(x_1, t_1, \mu^2)\Phi_{\bar{q}}^{\bar{p}}(x_2, t_2, \mu^2)\right. \\
&\left.\left. + \Phi_{\bar{q}}^p(x_1, t_1, \mu^2)\Phi_q^{\bar{p}}(x_2, t_2, \mu^2)\right] \overline{|\mathcal{M}(Q_q\bar{Q}_q \to b\bar{b})|^2}\right\}, \qquad (20)
\end{aligned}$$

where ϕ_1 is the azimuthal angle enclosed between the vectors $\vec{k}_{1T}$ and $\vec{q}_{1T}$, $\Delta\phi$ the one between $\vec{k}_{1T}$ and $\vec{k}_{2T}$,

$$\begin{aligned} x_{1,2} &= \frac{m_{1T}\exp(\pm y_1) + m_{2T}\exp(\pm y_2)}{\sqrt{S}}, \\ m_{1,2T} &= \sqrt{m^2 + k_{1,2T}^2}, \\ t_2 &= t_1 + k_{1T}^2 + k_{2T}^2 + 2k_{1T}k_{2T}\cos\Delta\phi - 2\sqrt{t_1}\left[k_{1T}\cos\phi_1 + k_{2T}\cos(\Delta\phi - \phi_1)\right]. \end{aligned} \quad (21)$$

In the massless limit, the b-quark transverse energy E_{1T} is given by $E_{1T} = k_{1T}$. The distribution in the $b\bar{b}$-invariant mass $M_{b\bar{b}}$ may be easily obtained from Eq. (20) by changing variables.

IV. RESULTS

Recently, the CDF Collaboration presented preliminary data on inclusive single b-jet production in $p\bar{p}$-collisions at Tevatron Run II [5]. The measurement was performed in the kinematic range $38 < k_T < 400$ GeV and $|y| < 0.7$. In Fig. 1, these data are compared with our predictions obtained in the QMRK approach as described in Secs. II and III. The contributions due to subprocesses (1) and (5) are shown separately. While the former may be evaluated from Eq. (18) as it stands, Eq. (20) must be integrated over k_{2T}, y_2, and $\Delta\phi$ in the latter case. Performing these integrations, care must be exercised to avoid double counting, to ensure the separation of the b jet from the underlying event, and to guarantee infrared safety. In the case of subprocess (1), the $\bar{b}$ quark is contained in the remnant of the hadron that emits the Reggeized b quark and is thus well separated from the final-state b quark detected in the central region of the detector. In order to avoid double counting, we therefore require for the $\bar{b}$ quark of subprocess (5) to satisfy $|y_2| < 4.5$. In fact, the cross section due to subprocess (5) is negligibly small for $|y_2| > 4.5$, so that the precise value of this cut-off is irrelevant. In order to implement the isolation of the b jet, we impose the acceptance cut $R_{\rm cone} > 0.7$, where $R_{\rm cone} = \sqrt{(y_1 - y_2)^2 + \Delta\phi^2}$, as in Ref. [5]. Since the lower bound of the k_{2T} integration is zero, we allow for the b-quark mass to be finite, $m_b = 4.75$ GeV. The renormalization and factorization scales are identified and chosen to be $\mu = \xi k_T$, where ξ is varied between 1/2 and 2 about its default value 1 to estimate the theoretical uncertainty. The resulting errors are indicated in Fig. 1 as shaded bands. We observe that the contribution due to subprocess (1) greatly exceeds the one due to

subprocess (5), by about one order of magnitude, and practically exhausts the full result. It nicely agrees with the CDF data throughout the entire k_T range. The QMRK results have to be taken with a grain of salt for $k_T \gtrsim 150$ GeV, where the average values of the scaling variables x_1 and x_2 in the unintegrated PDFs exceed 0.1, so that, strictly speaking, the QMRK approach ceases to be valid.

The CDF Collaboration also measured the inclusive $b\bar{b}$-dijet production cross section in Run II at the Tevatron [6]. The two jets were required to be in the central region of rapidity, with $|y_1|, |y_2| < 1.2$, to be separated by $R_{\rm cone} > 0.4$, and to have transverse energies satisfying the conditions $E_{1T} > 35$ GeV and $E_{2T} > 32$ GeV, where the jet with the maximal transverse energy is called the leading one. Given these acceptance cuts, the massless approximation is clearly applicable, so that $E_{iT} = k_{iT}$ and $y_i = \eta_i$, where η_i denote the pseudorapidities of the jets $i = 1, 2$. These data come as distributions in the leading-jet transverse energy E_{1T}, the dijet invariant mass $M_{b\bar{b}}$, and the azimuthal separation angle $\Delta\phi$. They are compared with our QMRK predictions in Figs. 2–4, respectively. The latter are evaluated from Eq. (20) including the contributions from subprocesses (5) and (10). The common scale is set to be $\mu = \xi k_{1T}$. In Figs. 2–4, these two contributions are shown separately along with their superpositions. The theoretical errors, estimated by varying ξ between 1/2 and 2, are indicated for the latter as shaded bands. We observe that the total QMRK predictions nicely describe all the three measured cross section distributions. The contributions due to subprocess (5) dominate for $E_{1T} \lesssim 200$ GeV and $M_{b\bar{b}} \lesssim 300$ GeV and over the whole $\Delta\phi$ range considered. The peak near $\Delta\phi = 0.4$ in Fig. 4 arises from the isolation cone condition.

The shaded bands in Figs. 1–4 only reflect the theoretical errors due to the uncertainties in the choices of the renormalization and factorization scales. Additional and possibly larger errors arise from our lack of knowledge of the unintegrated PDFs, which are, however, hard to quantify at this point.

V. CONCLUSIONS

We studied the inclusive hadroproduction of single b jets and $b\bar{b}$ dijets at LO in the QMRK approach, including subprocesses (1), (5), and (10) with Reggeized partons in the initial state. Despite the great simplicity of our formulas, our theoretical predictions turned

out to describe recent measurements of various cross section distributions by the CDF Collaboration in Run II at the Tevatron surprisingly well, without any ad-hoc adjustments of input parameters. By contrast, in the collinear parton model of QCD, such a degree of agreement can only be achieved by taking NLO corrections into account and performing soft-gluon resummation. In conclusion, the QMRK approach is once again [12] proven to be a powerful tool for the theoretical description of QCD processes in the high-energy limit.

Acknowledgements

The work of B.A.K. was supported in part by the German Federal Ministry for Education and Research BMBF through Grant No. 05H09GUE, by the German Research Foundation DFG through Grant No. KN 365/7–1, and by the Helmholtz Association HGF through Grant No. HA 101. The work of V.A.S. and A.V.S. was supported in part by the Federal Agency for Education of the Russian Federation under Contract No. P1338. The work of A.V.S. was also supported in part by the International Center of Fundamental Physics in Moscow and the Dynastiya Foundation.

---

[1] J. Binnewies, B. A. Kniehl, and G. Kramer, Phys. Rev. D **58**, 034016 (1998) [arXiv:hep-ph/9802231]; B. A. Kniehl, in *Proceedings of the 14th Topical Conference on Hadron Collider Physics: Hadron Collider Physics 2002*, Karlsruhe, 2002, edited by M. Erdmann and Th. Müller (Springer, Berlin, 2003), p 161, [arXiv:hep-ph/0211008]; in *Proceedings of the XVI International Workshop on Deep-Inelastic Scattering and Related Subjects (DIS 2008)*, London, England, 2008, edited by R. Devenish and J. Ferrando (Science Wise Publishing, Amsterdam, 2008), `http://dx.doi.org/10.3360/dis.2008.195` [arXiv:0807.2215 [hep-ph]]; B. A. Kniehl, G. Kramer, I. Schienbein, and H. Spiesberger, Phys. Rev. D **77**, 014011 (2008) [arXiv:0705.4392 [hep-ph]].

[2] V. S. Fadin and L. N. Lipatov, Nucl. Phys. **B406**, 259 (1993); Nucl. Phys. **B477**, 767 (1996) [arXiv:hep-ph/9602287].

[3] L. N. Lipatov, Nucl. Phys. **B452**, 369 (1995) [arXiv:hep-ph/9502308].

[4] L. N. Lipatov and M. I. Vyazovsky, Nucl. Phys. **B597**, 399 (2001) [arXiv:hep-ph/0009340].

[5] CDF Collaboration, T. Aaltonen *et al.*, CDF note 8418, 2006, URL: `http://www-cdf.fnal.gov/physics/new/qcd/QCD.html`.

[6] CDF Collaboration, T. Aaltonen *et al.*, CDF note 8939, 2007, URL: `http://www-cdf.fnal.gov/physics/new/qcd/QCD.html`.

[7] V. A. Saleev, Phys. Rev. D **78**, 034033 (2008) [arXiv:0807.1587 [hep-ph]]; Phys. Rev. D **78**, 114031 (2008) [arXiv:0812.0946 [hep-ph]].

[8] V. A. Saleev and D. V. Vasin, Phys. Lett. B **605**, 311 (2005) [arXiv:hep-ph/0411109].

[9] M. A. Kimber, A. D. Martin, and M. G. Ryskin, Phys. Rev. D **63**, 114027 (2001) [arXiv:hep-ph/0101348].

[10] A. D. Martin, R. G. Roberts, W. J. Stirling, and R. S. Thorne, Phys. Lett. B **531**, 216 (2002) [arXiv:hep-ph/0201127].

[11] V. A. Saleev, in *Proceedings of the XVII International Workshop on Deep-Inelastic Scattering and Related Subjects (DIS 2009)*, Madrid, Spain, 2009, edited by C. Glasman and J. Terron (Science Wise Publishing, Amsterdam, 2009), `http://dx.doi.org/10.3360/dis.2009.103`.

[12] B. A. Kniehl, D. V. Vasin, and V. A. Saleev, Phys. Rev. D **73**, 074022 (2006) [arXiv:hep-ph/0602179]; B. A. Kniehl, V. A. Saleev and D. V. Vasin, Phys. Rev. D **74**, 014024 (2006) [arXiv:hep-ph/0607254]; in *Proceedings of the 15th International Workshop on Deep-Inelastic Scattering and Related Subjects (DIS 2007)*, Munich, Germany, 2007, edited by G. Grindhammer and K. Sachs (Science Wise Publishing, Amsterdam, 2007), `http://dx.doi.org/10.3360/dis.2007.169`; B. A. Kniehl, A. V. Shipilova, and V. A. Saleev, Phys. Rev. D **79**, 034007 (2009) [arXiv:0812.3376 [hep-ph]].

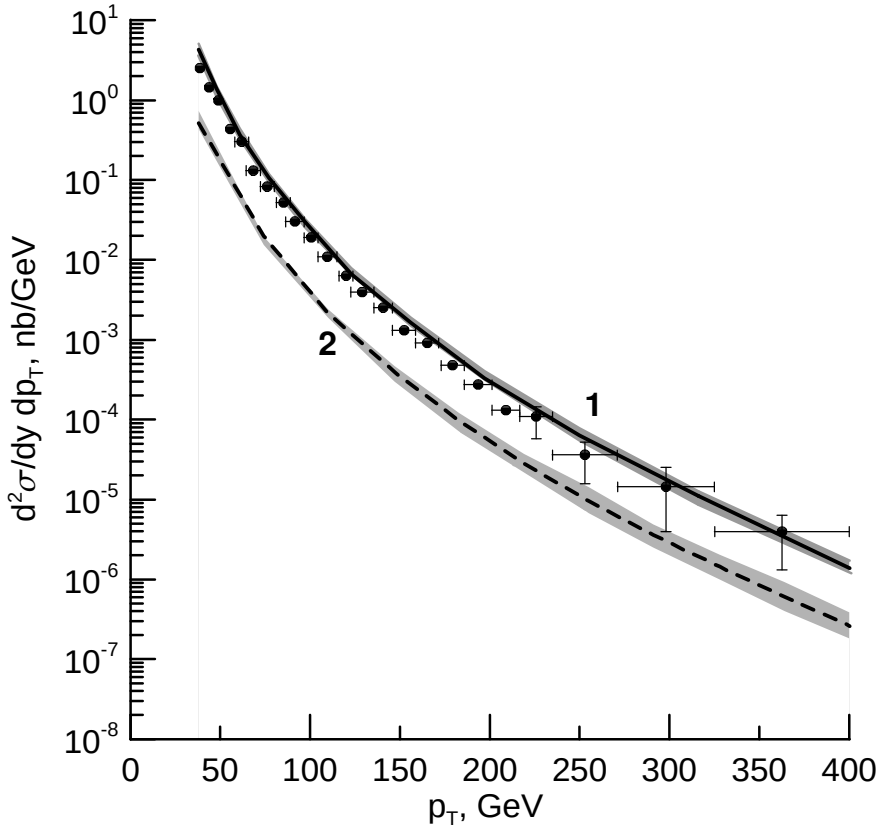

FIG. 1: The transverse-momentum distribution of inclusive single b-jet hadroproduction measured by the CDF Collaboration at Tevatron Run II [5] is compared with the QMRK predictions due to subprocesses (1) 1 and (5) 2. The shaded bands indicate the theoretical uncertainties.

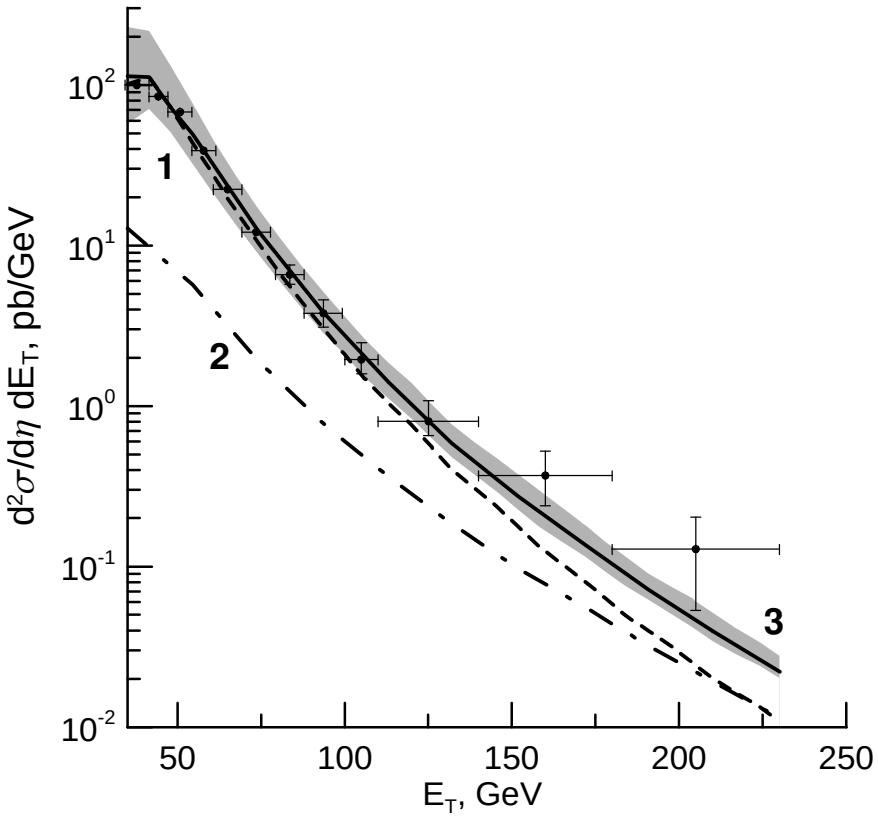

FIG. 2: The leading-jet transverse-energy distribution of inclusive $b\bar{b}$-dijet hadroproduction measured by the CDF Collaboration at Tevatron Run II [6] is compared with the QMRK predictions due to subprocesses (5) 1, (10) 2, and their sum 3. The shaded band indicates the theoretical uncertainty on the latter.

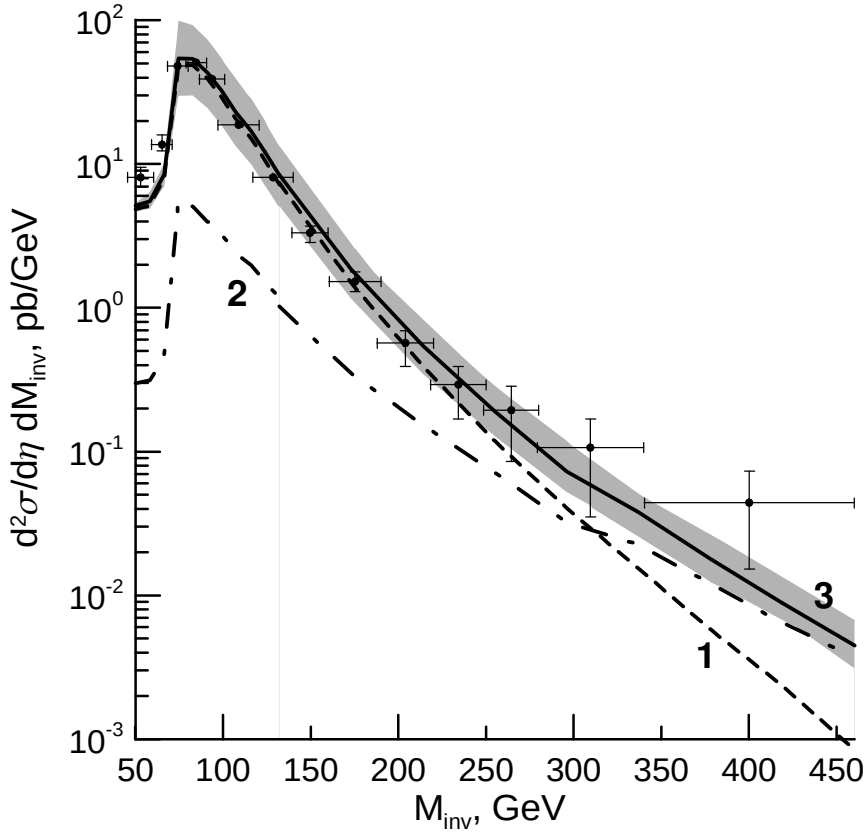

FIG. 3: The dijet-invariant-mass distribution of inclusive $b\bar{b}$-dijet hadroproduction measured by the CDF Collaboration at Tevatron Run II [6] is compared with the QMRK predictions due to subprocesses (5) 1, (10) 2, and their sum 3. The shaded band indicates the theoretical uncertainty on the latter.

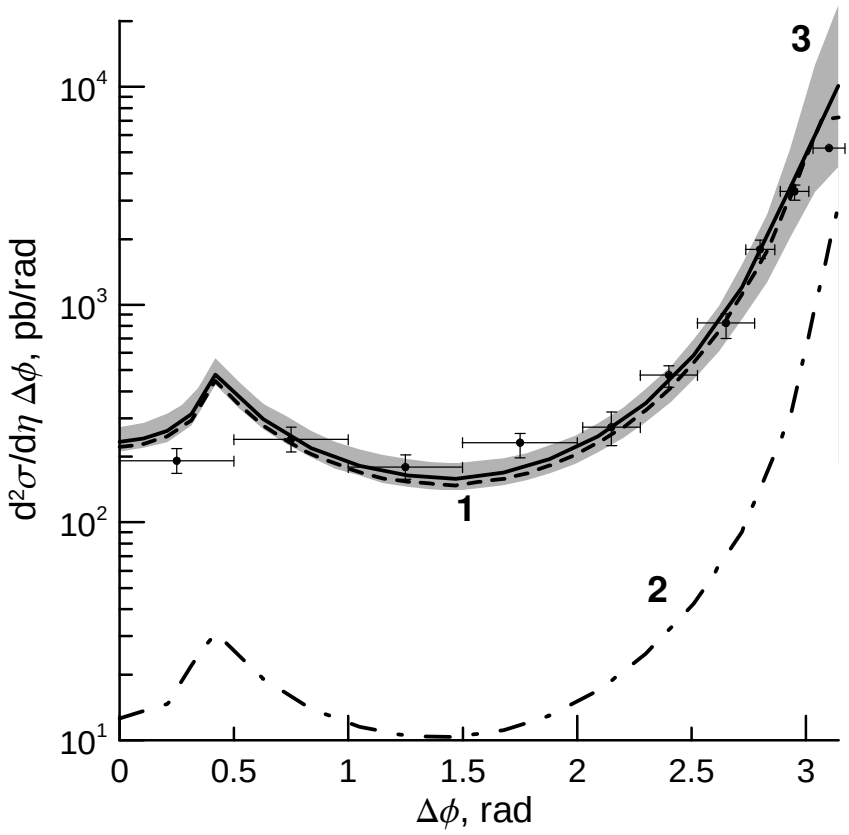

FIG. 4: The azimuthal-separation-angle distribution of inclusive $b\bar{b}$-dijet hadroproduction measured by the CDF Collaboration at Tevatron Run II [6] is compared with the QMRK predictions due to subprocesses (5) 1, (10) 2, and their sum 3. The shaded band indicates the theoretical uncertainty on the latter.